MIMO Techniques for Wireless Terabits Systems under sub-THz Channel with RF Impairments

Majed Saad, Ali Chamas Al Ghouwayel, Hussein Hijazi, Faouzi Bader, Jacques Palicot

MIMO Techniques for Wireless Terabits Systems under sub-THz Channel with RF Impairments

Majed Saad[†], Ali Chamas Al Ghouwayel[§], Hussein Hijazi[§], Faouzi Bader[†*] and Jacques Palicot[†]

[†]IETR/CentraleSupélec, Rennes Campus Cesson-Sévigné, France
[§]School of Engineering, Lebanese International University LIU, Lebanon
[*]ISEP, 28 rue N-D des Champs, 75006 Paris, France
majed.saad@ieee.org,{ali.ghouwayel, hussein.hijazi}@liu.edu.lb, faouzi.bader@isep.fr, jacques.palicot@supelec.fr

***Abstract*—Multiple-Input Multiple-Output (MIMO) systems and sub-TeraHertz (sub-THz) bands are being considered for the development of ultra-high data rate applications in beyond 5G. However, sub-THz band suffers from many technological limitations and severe RF-impairments such as low output power, limited resolution of high-speed ADCs, and important Phase Noise (PN) introduced by the Local Oscillator (LO). In this paper, MIMO Spatial Multiplexing (SMX) and Generalized Spatial Modulation (GSM) are compared from different perspectives while considering the sub-THz impairments. The effect of PN has been investigated for both systems in sub-THz channels using uniform linear and rectangular antenna arrays. The comparison is also performed in terms of Peak-to-Average-Power-Ratio (PAPR), power consumption, detection complexity and transmitter/receiver cost. In addition, the link budget and the system power consumption is estimated for both systems. The obtained results reveal that, when low order modulation schemes like QPSK is used, GSM outperforms SMX by a gain ranging from 4 up to 6.2 dB with a throughput rate reaching 0.5 Tbps that leads to 3.25 dB power gain with medium PN and non-coherent detection. Thus enforcing the GSM to be a promising candidate for ultra-high wireless data rate communication in sub-THz bands.**

***Index Terms*—Beyond 5G, millimeter wave (mmWave), sub-Terahertz systems (sub-THz), MIMO, spatial multiplexing, spatial modulation, Generalized Spatial Modulation (GSM), Index Modulation (IM), Phase Noise (PN), sub-Terahertz MIMO channel.**

I. Introduction

Millimeter wave (mmW) and sub-TeraHertz (sub-THz) bands are considered for beyond 5G ultra-high data rate scenarios [1]. In addition, Multiple-Input Multiple-Output (MIMO) systems with Spatial Multiplexing (SMX) were considered in many standards to increase the data rates, and recently Index Modulation (IM) techniques are introduced to enhance the spectral efficiency and/or power efficiency. Generalized Spatial Modulation (GSM) [2] is an another possible solution for future high-data rates applications, where a low power Terabits (Tbps) system can be achieved using GSM with power efficient single carrier modulations in spatially correlated/uncorrelated Rayleigh and Rician channels [3].

The research leading to these results received funding from the French National Research Agency under Grant Agreement no. ANR-17-CE25-0013 within the frame of the project BRAVE. We would like to thank CNRS GdR-ISIS for the research mobility grant, BRAVE project partners: Siradel for providing the sub-THz MIMO channels from their ray-based channel simulation and CEA-Leti for the suitable sub-THz phase noise model.

In the context of BRAVE project [4], we target to explore the sub-THz bands (90-200 GHz) for wireless Tbps communication. The RF-impairments increase at high frequencies and the signal propagation in sub-THz channel suffers from high atmospheric attenuation and high sensitivity to small environment details [10]. The major RF-impairments in sub-THz band are the Phase Noise (PN) introduced by the LOs, the low output power and the limited resolution of low-power high-speed Analog-to-Digital Converters (ADCs).

In this paper, a complete analysis is provided for SMX and GSM subjected to major sub-THz limitations and RF-impairments. To the best of our knowledge, this is the first paper that considers the performance analysis of GSM systems subjected to PN effects over sub-THz channels. This performance analysis includes a comparison with SMX systems in terms of performance, robustness to PN, computational complexity, cost, Peak-to-Average Power Ratio (PAPR), link budget and power consumption. The paper is organized as follows. In section II, SMX and GSM systems are presented, whereas in section III sub-THz and RF impairments are discussed. Section IV illustrates the results of the SMX and GSM comparisons from different perspectives and discusses the feasibility of both systems for ultra-high wireless communication in sub-THz band. Finally, concluding remarks are given in Section V.

The notations used in this paper are as follows. Matrices and vectors are represented by a bold capital and small letters respectively. $\lfloor . \rfloor$ represents the floor function. $\|.\|$ stands for the Frobenius norm. $(.)^T$ is used to denote the transpose of a matrix. $\binom{x}{y}$ represents the binomial coefficient. $\mathcal{CN}(\mu, \sigma^2)$ and $\mathcal{N}(\mu, \sigma^2)$ denotes the complex normal and real normal distribution respectively of a random variable having mean μ and variance σ^2.

II. Preliminaries

A. MIMO Spatial Multiplexing

Consider a MIMO Spatial Multiplexing (SMX) system with N_t transmit antennas (TAs) and N_r receive antennas (RAs) where $N_r \geq N_t$. Different M-ary Amplitude-Phase Modulation (APM) symbols are transmitted simultaneously

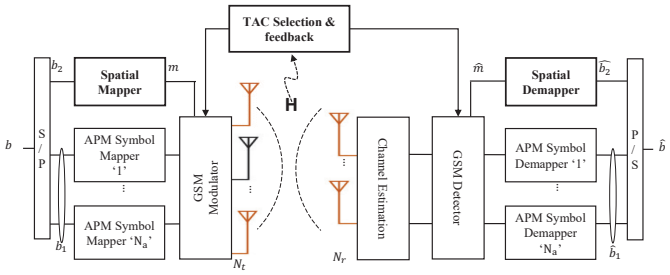

Fig. 1: System model of GSM with TAC selection

from the different TAs. Thus, the number of bits per SMX symbol is expressed as:

$$\mathcal{L}_{\mathcal{SMX}} = N_t \log_2(M). \tag{1}$$

The received signal vector $\mathbf{y}_1$ is expressed as:

$$\mathbf{y}_1 = \mathbf{H}.\mathbf{x}_{SMX} + \mathbf{n}, \tag{2}$$

$\mathbf{H} = [\mathbf{h}_1, ..., \mathbf{h}_{N_t}]$ is the $N_r \times N_t$ MIMO channel matrix where $\mathbf{h}_i$ is the column vector of N_r elements, $\mathbf{x}_{SMX} = [x_1, \ldots, x_{N_t}]^T$ is the transmitted vector that contains N_t different APM symbols, $\mathbf{n}$ is $N_r \times 1$ channel noise vector and its n_r elements are complex Gaussian variables, independent and identically distributed (i.i.d.), with zero-mean and variance σ_n^2, i.e, $\mathcal{CN}(0, \sigma_n^2)$ for $r = 1, \ldots, N_r$. The energy of the transmitted APM symbols are normalized to unity.

B. Principle of GSM

GSM system conveys information bits in the signal domain as in SMX system, but additional bits are conveyed in the spatial domain by means of IM [2]. Such GSM system consists of N_t TAs where only N_a TAs are activated at each symbol period to transmit different M-ary APM symbols as depicted in Fig. 1. Consequently, the possible number of Transmit Antenna Combinations (TACs) is then listed as a combination C_{Nt}^{Na} where the number of legitimate TACs is $N_{TAC} = 2^{\lfloor log_2(C_{Nt}^{Na}) \rfloor}$, and by indexing the different legitimate TACs, GSM conveys additional information bits by the index of TAC ($\log_2(N_{TAC})$ spatial bits per GSM symbol). Thus, the total number of bits per GSM symbol is given by:

$$\mathcal{L}_{GSM} = \log_2(N_{TAC}) + N_a.\log_2(M). \tag{3}$$

Note that only N_{TAC} are used from C_{Nt}^{Na} to keep the spatial bits length as an integer number and the other possibilities are marked as illegal TACs. In the following, we will consider the enhanced GSM system that selects the optimal legitimate TACs sets using the channel side information [5] and the best effort gray spatial-bit mapping (Index-to-Bit mapping) according to [6] to achieve the optimal GSM performance.

At the receiver end, the signal is represented as

$$\mathbf{y}_2 = \mathbf{H}.\mathbf{x}_{GSM} + \mathbf{n}, \tag{4}$$

where $\mathbf{x}_{GSM}$ is the GSM symbol vector of N_a different M-ary APM symbols transmitted through the active TAs according to the index of activated TAC.

Note that SMX is a special case of GSM system where all TAs are activated and the spatial domain does not convey any information bits.

C. Optimal Detection

The maximum-likelihood (ML) detector for SMX is able to detect all the N_t transmitted APM symbols by an exhaustive search over all possible transmit vectors. Similarly, the ML detection for GSM is performed to detect jointly the activated TACs and the N_a APM symbols:

$$\widehat{\mathbf{x}} = arg \min_{\mathbf{x} \in \chi} \|\mathbf{y} - \mathbf{H}.\mathbf{x}\|^2 . \tag{5}$$

where χ contains all possible TACs and GSM vectors. Note that many detection methods are proposed for GSM and SMX to reduce the high complexity of ML detector especially with large number of transmitted APM symbols of high modulation order. However, in this paper, we will consider the ML detection for a fair comparison between the GSM and the SMX systems with optimal performance.

III. Sub-Terahertz Channel and Impairments

In this section, the main sub-THz band impairments and challenges are addressed.

For high frequency broadband systems, the non-linearity of analog components used in Radio-Frequency (RF) front ends gives increased challenges in the modeling of circuits and in anticipating the compensation measures required for performance improvements. The RF front end is composed of all components between the antenna and the digital baseband system of a transceiver, namely mixer or modulator, phase shifter, and Power Amplifier (PA). Sub-THz bands suffer from many RF challenges, especially for low cost implementation, and they can be summarized as follows:

- Efficiency and achievable transmit output power are low compared to sub-GHz bands, where the maximum achievable output power is in the order of 10 dBm.
- Non-linearity effect of the PA and electronics components.
- Medium to strong Phase noise of the LO that leads to significant degradation in Signal-to-Noise Ratio (SNR) and limits both Bit-Error Rate (BER) performance and throughput rate.
- High power consumption and limited resolution for ultra-high sampling rate for ADCs [7].

In addition, the channel at sub-THz bands suffers from high atmospheric attenuation and very strong obstruction losses (from walls, vegetation, furniture, etc.), and high sensitivity to the environment details (small objects, surface roughness, etc.). For clarification, most surfaces that appear smooth for microwave frequencies leads to significant diffuse scattering and strong specular reflections for sub-THz frequencies [8]. In this paper, we focus on short-range scenario such as kiosk or hot-spot where the atmospheric attenuation is irrelevant.

A. Sub-Terahertz Phase noise model

It is well known that practical oscillator can never generate a pure sinusoid and the PN increases with the carrier frequency. Thus, the sub-THz communication system should be analyzed under this impairment since neglecting its impact is no more tolerable as in sub-GHz systems.

In general, the analysis of PN impact on MIMO systems is dependent on the RF architecture where there are mainly two LO setups: Distributed Oscillators (DO), Centralized or Common Oscillator (CO). The main difference is that each antenna in the DO setup has its own LO while in the CO setup all antennas at the transmitter\receiver are connected to a common LO. Consequently, all parallel streams in CO has the same PN while the DO suffers from different phase and amplitude distortions.

The PN model is widely investigated where the PN in general is modeled by two main models: Gaussian PN (uncorrelated PN) and Wiener PN (correlated PN). The wiener model is more accurate since it includes the cumulative PN (correlated term) due to the integration step of the Phase Locked Loop (PLL). However, wiener PN process becomes negligible compared to the Gaussian for wide-band systems where the oscillator corner frequency f_c is small compared to the system bandwidth [9]. Thus uncorrelated Gaussian PN model is more appropriate for sub-THz bands. Note that the uncorrelated model remains valid when the following condition is satisfied [9]:

$$N_s.f_c^2.T^2 \leq \frac{\ln(2)}{2\pi^2}, \tag{6}$$

where N_s is the number of symbols per frame, f_c is the corner frequency of the oscillator and T is the symbol period. It is clear that a careful communication system design can limit the wiener effect by selecting the appropriate N_s and T.

The received baseband vector of an equivalent $N_r \times N_t$ MIMO system with phase noise can be expressed as:

$$\tilde{\mathbf{y}} = \Phi_r \mathbf{H} \Phi_t \mathbf{x} + \mathbf{n}, \tag{7}$$

where Φ_t and Φ_r are the $N_t \times N_t$ and $N_r \times N_r$ diagonal matrices of phase noise from the transmitter and receiver oscillators respectively. These phase noise matrices can be represented as follows:

$$\Phi_t = \text{diag}\left([e^{j\theta_1^{Tx}}, ..., e^{j\theta_{N_t}^{Tx}}]^T\right) \tag{8}$$

$$\Phi_r = \text{diag}\left([e^{j\theta_1^{Rx}}, ..., e^{j\theta_{N_r}^{Rx}}]^T\right), \tag{9}$$

where θ_i^{Tx} and θ_j^{Rx} represent the PNs at the i^{th} TA and j^{th} RA respectively that can be described in sub-THz band by a truncated Gaussian distribution $\mathcal{N}(0, \sigma_g^2)$ with zero-mean and variance σ_g^2 similar to SISO PN model described in [9]. In the DO setup, $\theta_i^{Tx} \neq \theta_j^{Tx}$ and $\theta_i^{Rx} \neq \theta_j^{Rx}$ for all $i \neq j$. However, in the CO setup with independent oscillators for Tx and Rx sides (same oscillator is used for all antennas on each side but different oscillators for the Tx and Rx), $\theta_i^{Tx} = \theta^{Tx}$ for all $i = 1, ..., N_t$ and $\theta_j^{Rx} = \theta^{Rx}$ for all $j = 1, ..., N_r$. Thus, the received signal in the CO setup can be simplified to:

$$\tilde{\mathbf{y}} = e^{j\theta^{Tx}} e^{j\theta^{Rx}} \mathbf{H}\mathbf{x} + \mathbf{n} \tag{10}$$

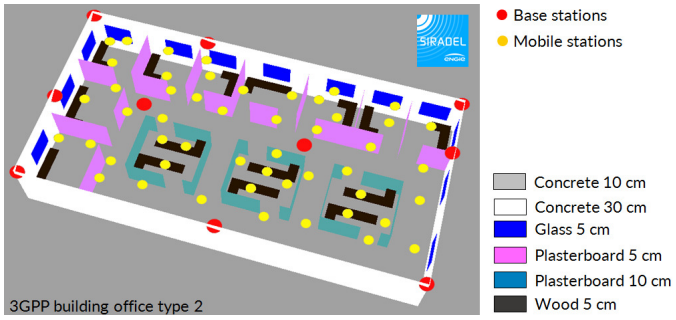

Fig. 2: In-office scenario environment [10]

B. Sub-THz MIMO Channel

A ray-based deterministic channel modeling for sub-THz Band (mainly between 90-200 GHz) is presented in [10]. It is worth mentioning that the propagation channel model in [10] considers the material properties, gaz attenuation and the impact of furniture that leads to more obstructions along the propagation paths and new scattered paths. In addition, it characterizes the main channel properties such as path loss and delay spread for LOS, NLOS with vegetation and NLOS cases for indoor in-office and outdoor in-street scenarios. In the following, we will focus on the downlink hotspot (or kiosk) indoor scenario where the Access Points (AP), acting as transmitters, and the Mobile Stations (MS), acting as receivers, are equipped with N_t and N_r isotropic antennas respectively in the positions depicted in Fig. 2. Therefore, the MIMO propagation channels are obtained using the simulator for ray-based deterministic channel modeling. The MIMO channels are obtained with different array geometry such as Uniform-Linear-Array (ULA) and Uniform-Rectangular-Array (URA). Note that an antenna elements separation of 4λ, where λ is the wavelength, is considered to reduce the effect of spatial correlation and thus enhance MIMO communication.

IV. Results and Discussions

In this section, the performance of the MIMO SMX and GSM subjected to sub-THz impairments will be studied using the sub-THz channel model described in previous section. Firstly, we will show the impact of PN in DO setup, considered as worst case, over MIMO sub-THz channels on both GSM and SMX systems for an indoor ultra-high data rate scenario. The system comparison is performed with different PN levels (low $\sigma_g^2 = 0.001$, medium $\sigma_g^2 = 0.01$, strong $\sigma_g^2 = 0.1$) without applying any phase noise mitigation technique. In our comparison, we consider the sub-THz indoor MIMO channels with a separation distance between MS and AP going from 2 to 8m, i.e. an average distance of 5m. For a fair comparison, both systems GSM and SMX are compared under the same spectral efficiency, which requires either the same modulation

schemes with SMX and GSM or the same number of activated TAs. We cannot conserve the same values for both variables because SMX needs to accommodate the virtual bits conveyed in GSM by increasing one of these parameters. The optimal ML detection is used along with the same number of RAs N_r. In the following, we will consider different systems with 12 bits per channel use (bpcu): QPSK-GSM with $N_t = 10$ and $N_a = 3$, QPSK-SMX with $N_t = 6$ and 16QAM-SMX with $N_t = 3$.

A. Performance under realistic MIMO sub-THz channel and PN

This sub-section compares SMX and GSM performance in sub-THz channel subjected to different PN levels and using different antenna array geometry. Fig. 3 shows clearly that QPSK-GSM outperforms SMX subjected to any PN level. For example, a gain of 4 dB is obtained using QPSK-GSM as compared to QPSK-SMX system, and which goes to 6.8 dB when compared to 16QAM-SMX with $N_r = 6$ at low PN as shown in Fig. 3.a. However, these values of gain are respectively reduced to 2 and 4.2 dB when $N_r = 10$ as shown in Fig. 3.b. Note that QPSK-SMX in sub-THz channels performs better than 16QAM-SMX for same spectral efficiency in all cases. Moreover, the performance gain of QPSK-GSM is much higher at medium PN when compared with QPSK-SMX, and becomes more advantageous when compared to 16QAM-SMX, where we notice that the high M-ary QAM schemes are very sensitive to PN. Thus, GSM is more robust to PN since the amount of information being conveyed and contained in the phase of the complex symbols (QPSK or QAM) is less as compared to SMX, while a part of this information is conveyed through the virtual bits (less sensitive to the PN effect). Note that both systems, without phase noise mitigation techniques, suffer from a high error floor when subjected to strong PN in sub-THz channels. The simulation results with URA geometry are shown in Fig. 4, where similar conclusion on the obtained gain can be drawn with the difference that all systems require a slightly larger SNR due to higher spatial correlation between antennas.

Therefore, GSM can survive at low to medium PN in sub-THz channel but more research is required to enhance GSM performance with strong PN channel. It is worth mentioning that the performance can be enhanced in PN channel by using PN robust modulations (e.g. spiral QAM [11],...) and/or differential schemes, powerful channel coding technique and special detector/equalizer designed specifically for PN channel.

B. ML Computational Complexity

In this subsection, SMX and GSM receivers are compared from the detection complexity point of view. The ML complexity is measured by the number of real multiplications performed because the hardware complexity of the addition is negligible compared to the multiplications. The number of Euclidean distances being calculated in the ML detector for SMX is $M^{N_t} = 2^{\mathcal{L}_{SMX}}$ while it is $N_{TAC}M^{N_a} = 2^{\mathcal{L}_{GSM}}$ for GSM. The number of non-zero real multiplications in the matrix multiplication $H.x$ is $4N_r.N_t$ for SMX and $4N_r.N_a$ for GSM since each complex multiplication is 4 real multiplications and 2 real additions. In addition, the Frobenius norm contains $2N_r$ real multiplications, so the total ML detector complexity for SMX and GSM in terms of real multiplications can be expressed as:

$$\mathcal{C}_{SMX} = 2^{\mathcal{L}_{SMX}+1}(2N_t + 1)N_r \tag{11}$$

$$\mathcal{C}_{GSM} = 2^{\mathcal{L}_{GSM}+1}(2N_a + 1)N_r. \tag{12}$$

It is clear that GSM and SMX have same detector computational complexity when they have same system spectral efficiency $\mathcal{L}_{SMX} = \mathcal{L}_{GSM}$, number of activated TAs and RAs but with higher modulation order in SMX system. However, SMX suffers from higher computational complexity when the number of activated TAs in SMX $N_t > N_a$ is increased to maintain the same efficiency and modulation order as GSM for a better robustness to PN using low modulation order. The complexity of SMX in both configurations compared to GSM with same spectral efficiency (12bpcu) is illustrated in Fig. 5, where MIMO QPSK-SMX is 1.86 times more complex than QPSK-GSM.

C. Discussion

In this sub-section, we will complete our analysis by considering other important factors for sub-THz communication. MIMO systems in sub-THz bands require using low order modulation schemes as QPSK for two reasons: 1) higher robustness to PN and 2) the limited resolution of ultra-high speed low power ADCs to few bits (limited quantization levels). Thus, low order modulation schemes with GSM or other IM techniques is required to achieve an ultra-high data rates.

When using the same modulation schemes, GSM and SMX have the same PAPR only if an RF antenna switching is applied after the PA. However, this switching causes spectral regrowth due to pulse time-truncation at each symbol period and thus reduces the spectral efficiency of GSM. A possible solution is to have full-RF chain Tx architecture ($N_{RF} \approx N_t$) that transmits the pulse tails when a TA is inactive. This solution leads to higher transmitter cost (for AP can be tolerated) and a higher PAPR compared to SMX since GSM PAPR highly depends on the modulation schemes and the number of inactive TAs. Note that the PAPR affects the PA efficiency and thus the system power consumption. This drawback of GSM can be mitigated by simple PAPR reduction techniques. As conclusion, the RF switching needed to be performed after the PA in order to maintain the same PAPR, induces a spectral efficiency decrease in the GSM transmitter which can be re-adjusted by using a full-RF architecture, i.e. more RF chains, along with PAPR reduction techniques compared to QPSK-SMX. This can be tolerated for the base stations\APs, and it is more appropriate for ultra-high data rates system since the RF-switching is no more needed and the spectral efficiency gain by IM is conserved.

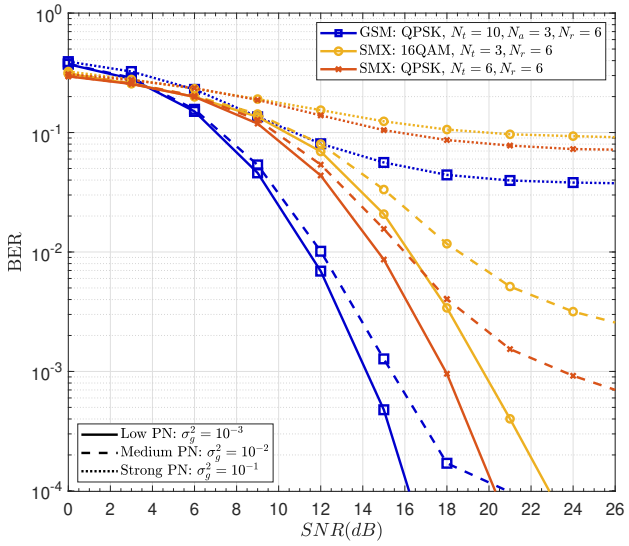

(a)

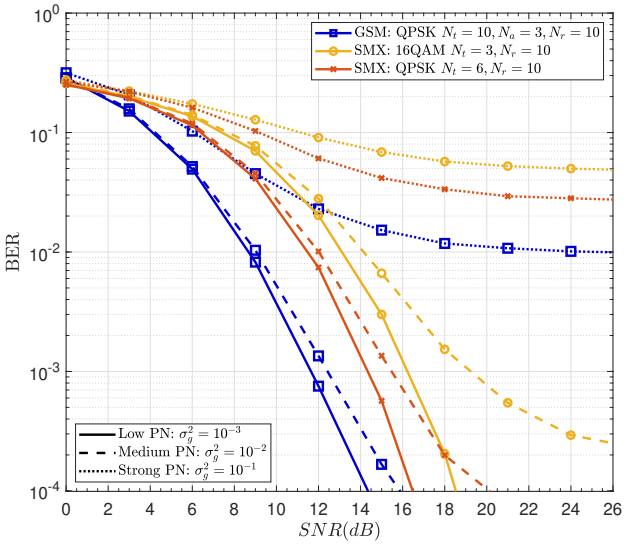

(b)

Fig. 3: BER performance of 12bpcu MIMO SMX and GSM systems subjected to different phase noise levels in DO setup. AP-MS mean distance is $d_{mean} = 5m$. ULA array geometry with 4λ antenna separation is used with (a) $N_r = 6$, (b) $N_r = 10$.

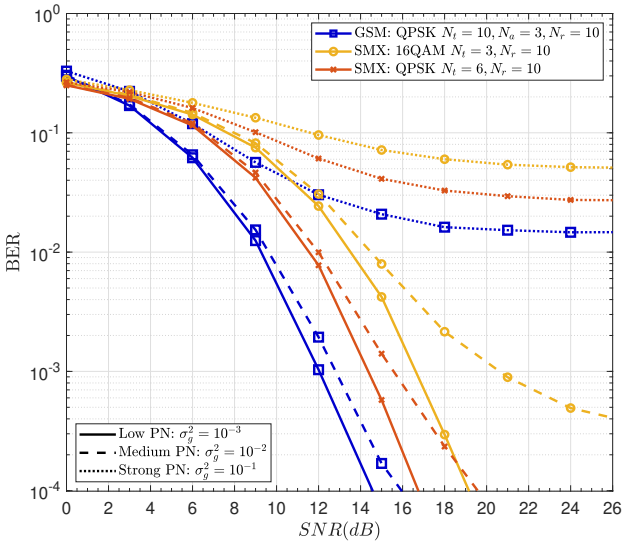

Fig. 4: BER performance of 12bpcu MIMO SMX and GSM systems subjected to different phase noise levels in DO setup. AP-MS mean distance is $d_{mean} = 5m$. URA array geometry with 4λ antenna separation is used with $N_r = 10$.

D. Link Budget

In this subsection, the link budget for SMX and full-RF GSM subjected to PN in indoor sub-THz channels for downlink ultra-high wireless data rates is presented. In this link budget estimation, the system configuration presented in Fig. 3b with medium PN is used to estimate the required transmit power for achieving the needed SNR at un-coded BER$= 10^{-4}$. The link budget, the estimated total power consumption and the data rates using GSM and SMX are presented in Table I with different values of total system bandwidth.

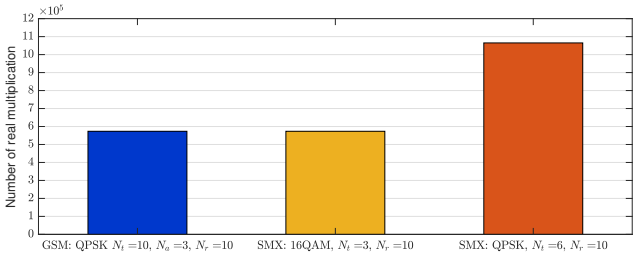

Fig. 5: ML detector computational complexity for GSM and SMX with same spectral efficiency 12bpcu.

In Table I, the required transmit power P_t with small distance communication is calculated from the required SNR according to the following parameters:

$N_{Thermal}$	$= 10\log_{10}(k.T.W) + 30$	dBm
N_{Floor}	$= N_{Figure} + N_{Thermal}$	dBm
Rx_{Level}	$= SNR + N_{Floor}$	dBm
$fspl$	$= 20\log_{10}(\frac{4\pi df_c}{c})$	dB
$EIRP$	$= fspl - G_r + Rx_{Level}$	dBm
P_t	$= EIRP - G_t$	dBm

where k, T, W, N_{Figure}, $fspl$, f_c, c, G_r/G_t and $EIRP$ are Boltzmann constant, the temperature in kelvin, the channel bandwidth, the noise figure, the free space path loss, the carrier frequency, the speed of light in vacuum ($c = 3 \times 10^8 m/s$), receive/transmit antenna gain, and the effective isotropic radiated power respectively. Furthermore, the power consumption is deduced based on the PA efficiency which is affected by the PAPR.

It is clear from Table I that GSM has a lower power consumption compared to SMX even when using full-RF GSM that suffers from higher PAPR and thus lower PA efficiency. Note that the required EIRP for both systems to reach AP-MS distance up to 8m is less than the maximum allowed EIRP

TABLE I: Link budget of SMX and GSM systems over sub-THz channels and subjected to medium PN.

Link Budget	GSM	SMX
Carrier frequency (GHz)	150.00	
Distance (m)	2 to 8	
Channel Bandwidth W (GHz)	0.50	
Spectral Efficiency (bpcu)	12	
Pulse Shaping: Rolloff	Root Raise cosine: 0.2	
Spectral efficiency (b/s/Hz)	10	
Data Rates per Channel (Gbps)	up to 6	
Required Transmit Power P_t (dBm)	-1.96 to 10.08	2.04 to **14.08**
Transmit antenna gain G_t (dBi)	15.00	
EIRP (dB)	13.04 to 25.08	17.04 to 29.08
$fspl$ (dB)	81.98 to 94.02	
Receive antenna gain G_r (dBi)	5.00	
Received power Rx_{level} (dBm)	-63.94	-59.94
Thermal noise (PSD) (dBm/Hz)	-174.00	
Noise figure N_{Figure} (dBm)	7.00	
Thermal noise $N_{Thermal}$ (dBm)	-86.94	
Noise floor N_{floor}	-79.94	
SNR with medium PN (dB)	16.00	20.00
Average PAPR (dB)	7.66	6.18
PA efficiency	0.32	0.38
Power consumption (dBm/channel)	2.99 to 15.03	6.24 to 18.28
12.5 GHz channel bounding (25 channels)		
Data Rates (Gbps)	~125	
Total Power consumption (dBm)	16.97 to 29.01	20.22 to 32.26
48 GHz channel bounding and aggregation (96 channels)		
Data Rates (Gbps)	~480	
Total Power consumption (dBm)	22.81 to 34.85	26.06 to 38.10

in regulations (40 dBm). In addition, the required transmit power for GSM is achievable using the existing electronic technology, while for SMX system it is 14.08 dBm for 8m AP-MS distance which is more than the currently available output power at sub-THz band.

In our example, PAPR after pulse shaping of QPSK-GSM is $1-2$ dB higher compared to QPSK-SMX, but GSM keeps a lower power consumption due to its lower SNR requirement for the same BER. For clarification, GSM requires 3.25 dB less than SMX system, that means less than half of the required power with SMX system. Moreover, the total power consumption and data rates are estimated with different total system bandwidths that are available in the band between 90 GHz and 175 GHz. SMX and GSM systems can reach up to 125 Gegabits per second (Gbps) and 480 Gbps (~0.5 Tbps) when the considered total system bandwidth, after channel aggregation and bounding, is 12.5 GHz and 48 GHz respectively with 0.2 pulse shaping rolloff factor. Therefore, if the residual PN before detection is in a medium level, the presented system QPSK-GSM can be considered as an appropriate solution for indoor ultra-high wireless data rates system in the sub-THz while having an acceptable AP power consumption between 0.2 and 3 Watts for 0.5 Tbps.

V. Conclusion

In this paper, GSM and SMX is compared from different perspectives subjected to realistic sub-THz impairments in an indoor environment. The simulations results reveal that MIMO GSM outperforms SMX for all PN levels in the sub-THz channels using ULA or URA array geometry with non-coherent detection. The performance gap increases with the increase in PN, where GSM outperforms SMX in terms of BER even when both systems use same modulation order. Among SMX systems, QPSK-SMX achieves better performance than 16QAM-SMX at the cost of higher detection complexity. The performance of higher order QAM-SMX is primarily limited due to higher sensitivity to PN. In addition, GSM system with non-coherent detection achieves good performance in the presence of low and medium PN, and a PN mitigation is required for strong PN case.

Finally, compared to SMX system, the GSM system with low modulation order offers better performance, lower complexity, lower power consumption (less than half compared to SMX) and higher robustness to PN and few-bits ADC resolution requirement, which make it a potential candidate for ultra-high data rates in sub-THz bands. However, full-RF GSM may suffers from higher transmitter cost and PAPR but it overcomes the ultra-fast RF switching issue and the spectral efficiency degradation. Moreover, we would like to highlight that low order modulation schemes are required to allow related systems to survive with sub-THz technological limitations, which imposes the use of spectral efficient IM techniques in order to achieve ultra-high data rates. Future work will focus on investigating MIMO joint detection-PN mitigation techniques and proposing novel IM domain.

References

[1] M. Saad, F. Bader, J. Palicot, Y. Corre, G. Gougeon, J-B Doré, "Beyond-5G wireless Tbps Scenarios and Requirements," French funded project-ANR-17-CE25-0013 BRAVE, Tech. Report BRAVE D1.0, 2018. [Online]. Available: https://hal.archives-ouvertes.fr/hal-01947363/document.

[2] J. Wang, S. Jia and J. Song, "Generalised Spatial Modulation System with Multiple Active Transmit Antennas and Low Complexity Detection Scheme," *IEEE Trans. Wireless Commun.*, vol. 11, no. 4, pp. 1605-1615, April 2012.

[3] M. Saad, F. Bader, J. Palicot, A. C. Al Ghouwayel, H. Hijazi, "Single Carrier with Index Modulation for Low Power Terabit Systems," IEEE Wireless Commun. and Netw. Conf. (WCNC), Marrakech, Morocco. Apr. 2019.

[4] French funded project-ANR-17-CE25-0013, "Back to Single-carrier for beyond-5G communications above 90 GHz-(BRAVE)," [Online]. Available: http://www.brave-beyond5g.com/.

[5] L. Xiao et al., "Transmit Antenna Combination Optimization for Generalized Spatial Modulation Systems," *IEEE Access*, vol. 6, pp. 41866-41882, 2018.

[6] M. Saad, F. Lteif, A. C. Al Ghouwayel, H. Hijazi, J. Palicot and F. Bader, "Generalized Spatial Modulation in Highly Correlated Channel," IEEE International Symposium on Personal Indoor and Mobile Radio Communications (PIMRC), Istanbul, Turkey, Sept. 2019.

[7] B. Murmann, "ADC Performance Survey 1997-2019," [Online]. Available: http://web.stanford.edu/ murmann/adcsurvey.html

[8] T. S. Rappaport et al., "Wireless Communications and Applications Above 100 GHz: Opportunities and Challenges for 6G and Beyond," *IEEE Access*, vol. 7, pp. 78729-78757, 2019.

[9] S. Bicaïs, J-B. Doré, "Phase Noise Model Selection for Sub-THz Communications," IEEE Global Communications Conference 2019, Waikoloa, United States, Dec 2019.

[10] G. Gougeon, Y. Corre, M. Aslam, "Ray-based Deterministic Channel Modelling for sub-THz Band," IEEE International Symposium on Personal Indoor and Mobile Radio Communications (PIMRC), Istanbul, Turkey, Sept. 2019.

[11] A. Ugolini, A. Piemontese and T. Eriksson, "Spiral Constellations for Phase Noise Channels," *IEEE Trans. Commun.*, vol. 67, no. 11, pp. 7799-7810, Nov. 2019.